Asymmetric nanowire SQUID: Linear current-phase relation, stochastic switching, and symmetries

A. Murphy and A. Bezryadin

Phys. Rev. B **96**, 094507 — Published 11 September 2017

DOI: 10.1103/PhysRevB.96.094507

Asymmetric nanowire SQUID: linear CPR, stochastic switching, and symmetries

A. Murphy[1] and A. Bezryadin[1]

[1]*Department of Physics, University of Illinois at Urbana-Champaign, Urbana, Illinois 61801, USA*

(Dated: February 28 28, 2017)

We study nanostructures based on two ultrathin superconducting nanowires connected in parallel to form a superconducting quantum interference device (SQUID). The measured function of the critical current versus magnetic field, $I_C(B)$, is multivalued, asymmetric and its maxima and minima are shifted from the usual integer and half integer flux quantum points. We also propose a low-temperature-limit model which generates accurate fits to the $I_C(B)$ functions and provides verifiable predictions. The key assumption of our model is that each wire is characterized by a sample-specific critical phase, ϕ_C, defined as the phase difference at which the supercurrent in the wire is the maximum. For our nanowires ϕ_C is much greater than the usual $\pi/2$, which makes a qualitative difference in the behavior of the SQUID. The nanowire current-phase relation is assumed linear, since the wires are much longer than the coherence length. The model explains single-valuedness regions where only one vorticity value, n_v, is stable. Also, it predicts regions where multiple vorticity values are stable because the Little-Parks (LP) diamonds, which describe the region of stability for each winding number n_v in the current-field diagram, can overlap. We also observe and explain regions in which the standard deviation of the switching current is independent of the magnetic field. We develop a technique that allows a reliable detection of hidden phase slips and use it to determine the boundaries of the LP diamonds even at low currents where $I_C(B)$ is not directly measurable.

I. INTRODUCTION

Superconducting quantum interference devices[1, 2] (SQUIDs) are known to be extremely sensitive to weak magnetic fields, and therefore various forms of superconducting loops have recently attracted significant attention[3–11]. Nanowire networks[12] and loops[13–20] are qualitatively distinct from networks of Josephson junctions and conventional SQUIDS. This is because nanowires can sustain superconductivity by themselves, up to their depairing current, and because they have a near linear current-phase relationship (CPR) at low temperatures [13, 21, 22], which can be multivalued [23]. Josephson junctions, on the other hand, obey a sinusoidal CPR, which is single-valued and has a critical phase of $\pi/2$, which is the phase difference when the critical current is achieved.

Nanowire SQUIDs have been used in important applications such as the detection of macroscopic quantum tunneling in magnetic systems with large spins[24]. Thus, some important applications of a nanowire SQUID demand very low temperatures. Yet virtually all models of nanowire SQUIDs are based on Ginzburg-Landau equations, which are valid only near the critical temperature. Thus, one goal of this paper is to develop a model which would be applicable for low temperatures. As will be discussed, we find such a model which provides excellent fits to our data and predicts hidden phase slips at low bias currents, which we observe.

The properties of unshunted conventional SQUIDs composed of two Josephson junctions are well known [2]. In the simplest case where the loop inductance is negligible, the critical current of the SQUID is a periodic, single-valued function of the magnetic field, and its maxima correspond to integer multiples of the flux quantum, while its minima occur at half flux quantum plus an integer number of flux quanta[2]. If the SQUID is asymmetric, i.e. if the critical currents of the two branches forming the SQUID are different, then the conditions listed above remain true, but the critical current modulation does not go all the way to zero at half flux quantum. The fact that the maxima and minima of the critical current versus magnetic field function $I_C(B)$ coincide with integer and half-integer normalized flux values is due to the sinusoidal nature of the CPR for each weak link and the associated critical phase of $\pi/2$.

Here we present experiments and propose a model for asymmetric nanowire SQUIDs in which the critical phase is significantly larger than $\pi/2$. This fact leads to the occurrence of multiple metastable states which differ by their winding number (vorticity), n_V. We elucidate the qualitative changes which the function $I_C(B)$ exhibits in such cases. The devices exhibit certain characteristics which make them qualitatively different from the conventional unshunted SQUIDs [2]. We observe that the critical current of the nanowire SQUID is multi-valued and its minima and maxima can shift strongly from the usual integer and half-integer flux quanta values. These features have been observed previously [14, 25–28]. We also observe that the general shape of the $I_C(B)$ curve is made of linear segments rather than being sinusoidal. At temperatures much lower than the critical temperature T_C, a linear CPR (and therefore a linear relationship between critical current and field) is both expected [2, 21–23, 29, 30] and has some experimental evidence [13, 15, 25–27].

Advanced computational simulations based on Ginzburg-Landau (GL) theory, which is known to be

valid at temperatures near the critical temperature T_C [31], have been used to simulate the critical current versus field dependence of nanowire loops previously [25, 27, 28]. While some of these computational models do calculate a piecewise linear or near-linear dependence of critical current on magnetic field [25, 27], these authors do not present theoretical analysis of cases in which the loop is asymmetric. Additionally, none plot theory on top of experimental data to allow direct comparison of the two. Here we propose a simple model, based on a linear CPR, which allows accurate fitting of the critical current versus field dependence. The model predicts the multi-valuedness, shifts in maxima and minima, and the linearity of the $I_C(B)$ function. Thus, we confirm theoretical predictions that the CPR of a thin wire is linear at very low temperatures [2, 21, 22]. We address asymmetric systems quantitatively and plot theoretical curves on top of experimental data for direct comparison.

We also observe and discuss unusual plateaus in the standard deviation of the switching current distribution. Furthermore, we observe that the regions of stability of the vorticity, namely the Little-Parks diamonds [27, 32, 33], can overlap significantly, thus generating multivaluedness of the critical current and of the vorticity at a fixed magnetic field. Yet we find some magnetic field - bias current parameter regions, which we call unique-vorticity diamonds, in which only one vorticity is stable. These results open doors to vorticity-manipulation experiments. We observe that the critical current versus field function $I_C(B)$ is symmetric with respect to the origin, if both positive and negative branches are included. This fact is explained within our linear-CPR model of a nanowire SQUID. Finally, we observe the presence of hidden phase slips, i.e. phase slips which are not accompanied by the switching of the device to the normal state, as predicted in our model.

II. EXPERIMENT

All three measured nanowire SQUIDs, Device 7715s1 (Fig. 1), Device 51215s3 and Device 31414s1 are produced by a molecular templating method [34, 35]. In brief, the nanowires were made by depositing carbon nanotubes across a 100 nm - 200 nm trench on a Si chip coated with a bilayer of SiO_2 and SiN. A layer of $Mo_{75}Ge_{25}$ was sputtered on the entire chip coating both the carbon nanotubes and the SiN surface. This layer was 18 nm thick for Device 7715s1, 17 nm thick for Device 51215s3 and 10 nm thick for Device 31414s1. This process creates both the $Mo_{75}Ge_{25}$ nanowires and the wide electrodes connected to them simultaneously; thus contact resistance does not occur. Contact pads and electrodes were then patterned by photolithography such that after etching with H_2O_2, only the two desired nanowires remained as weak superconducting links between the electrodes (Fig. 1). The width of the electrodes is 20 μm.

Each device consists of two nonidentical nanowires which are connected in parallel, forming an asymmetric superconducting loop (Fig. 1). The bias current flows from one of these electrodes, through the pair of nanowires, to the second electrode. One nanowire of Device 7715s1 is 42 nm wide and 140 nm in length, and the other one is 26 nm wide and 158 nm in length. The nanowires are separated by 2.5 μm. Device 51215s3 consists of a 29 nm wide and 190 nm long nanowire, separated from a 19 nm wide and 170 nm long nanowire by a distance 1.3 μm. Device 31414s1 consists of a 35 nm wide and 225 nm long wire, separated from a 23 nm wide and 216 nm long wire by a distance of 2.6 μm.

Device 7715s1 is measured at 320 mK in a He3 system, and all devices are measured at and above 1.5 K in a He4 cryostat. A current biasing is achieved by placing larger resistors in series with the device and a sinusoidal voltage source (function generator DS360). Two resistors have been used, 1 kΩ and 47 kΩ. Current is calculated using Ohm's law by measuring the voltage across the 1 kΩ resistor whereas the voltage on the sample is measured on the contact pads, which are connected to the superconducting electrodes of the SQUID. The bias current is a sinusoidal function of time, the frequency being 1.1 Hz (for Device 7715s1 in the He3 measurements), or 3.5 Hz (Device 7715s1 and Device 51215s3 in the He4 setup) or 11 Hz (Device 31414s1 in the He4 setup). The voltage-current (V-I) curves have been acquired using LabVIEW. At low bias linear V-I curves have been observed and the slope was determined, providing the sample resistance.

As temperature is decreased, the resistance of each device shows two transitions (Fig. 2a). At the higher temperature transition, the contact pads and electrodes become superconducting, while at the lower temperature transition the nanowires become superconducting. The temperature at which the nanowires becomes superconducting is taken as the critical temperature T_C.

Let us now discuss the voltage-current (V-I) dependence of our SQUIDs (Fig. 2b). At temperatures sufficiently below T_C, as the current is increased from zero, the voltage across the device is initially zero, but at some critical value of the applied current the voltage suddenly jumps from zero to a large value of the order of tens of mV (Fig. 2b). Such a sudden jump indicates that the device switches to the normal (i.e., non-superconducting) state. The current at which this transition takes place is recorded as the critical current, I_C, of the SQUID device. As shown in Fig. 2b there are two such critical currents, one at positive applied bias, I_{C+}, and one at negative applied bias, I_{C-}, for each complete V-I curve. Note that the V-I curve has a clear hysteresis. This is because, after a switching event, the device becomes trapped in the normal state due to Joule heating. As the current is re-

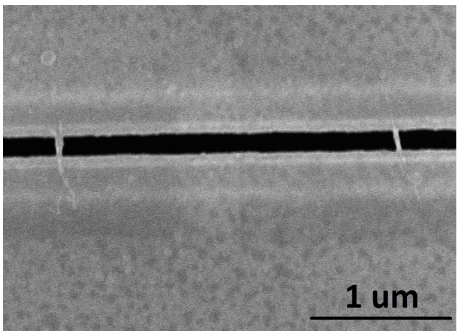

FIG. 1: An SEM image of Device 7715s1. Two nanowires (gray) lay across a 140 nm wide trench (black). The distance between the wires is 2.5 μm. The superconducting electrodes appear as the gray areas above and below the nanowires.

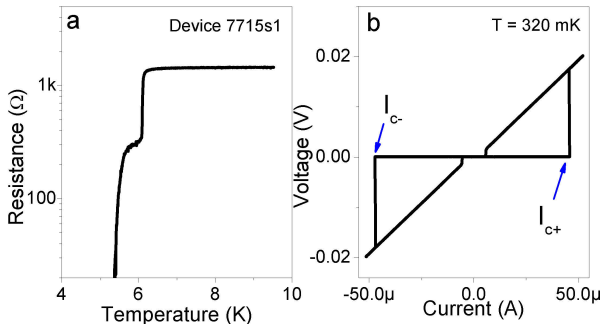

FIG. 2: a) The resistance of Device 7715s1 plotted vs temperature shows two transitions. The higher temperature transition occurs when the larger features of the device (the electrodes and contact pads) become superconducting. The lower temperature transition occurs when the nanowires become superconducting. b) The voltage vs current (V-I) curve is measured at temperatures far below the critical temperature. As current through the device is increased from zero, the voltage suddenly jumps at the critical currents (labeled on the plot as I_{C+} at positive applied bias current or I_{C-} at negative applied bias current). If the V-I curve is measured again, it would look qualitatively similar except that the voltage jump would occur at a somewhat different current. Thus, every measured V-I curve generates one particular value of the switching current.

duced significantly, the Joule heating diminishes and the device switches back to the superconducting state.

If we repeat the V-I curve measurement under the same conditions then there are two possibilities. First, if the vorticity of the loop is not changed then the new V-I curve will exhibit very similar positive and negative critical currents. A small difference might still be present since the measured critical current is sensitive to internal fluctuations of the supercurrent in the nanowires. Due to this, the measured critical current is sometimes called "switching current", simply because it is usually a little bit smaller than the true theoretical critical current, due to the fluctuations. The second possibility is that the vorticity of the loop will accept a different value as the current is reduced and the device switches back to its superconducting state. In this case, the measured critical currents of the new vorticity state may deviate significantly from the initial measurement. As will be discussed later, our experiments suggest that by cycling the device between the superconducting and normal states (by sweeping the current up and down) it is possible to cause a change in the winding number of the condensate on the loop. Yet, if the temperature stays low, the winding number does not change on its own.

In Figure 3a we plot the critical current (black dots) of the SQUID 7715s1 versus applied perpendicular magnetic field B. Each dot is obtained from a single V-I curve measurement. Multiple measurements of the critical current are taken at each value of magnetic field. Each V-I curve measured possesses one voltage jump at the positive critical current and one voltage jump at the negative critical current. If the measurement is repeated the jumps occur at different values of the current. The measured critical current values tend to cluster along certain lines on the B-I plane. Due to this, the resulting critical current plot is a multivalued periodic function of the magnetic field, composed of approximately linear segments and resembling a periodic sequence of diamonds. Note that a linear dependence of the critical current on the magnetic field has been observed previously [13, 15, 25–27].

The switching current versus field graph appears multivalued (Fig. 3) because the winding number of the order parameter (the vorticity) influences the value of the critical current. And the vorticity can fluctuate from one measurement to the next one because when the current is swept above its critical value the superconductivity is destroyed and the winding number is erased. Then, when the current is reduced back to zero, superconductivity occurs again and a new vorticity value is created. If the vorticity would always be equal to the value minimizing the energy then we would not see the multivalued graph of Fig. 3; the result would be single-valued. Yet, due to thermal fluctuations, the SQUID loop can freeze into a vorticity which is somewhat different from the value minimizing the energy. Such freezing of different vorticity values appears similar to the one observed in the experiments demonstrating Kibble-Zurek mechanism in superconducting rings [36].

In Fig. 3b, the positive critical current I_{C+} is compared to the negative critical current I_{C-}, which was multiplied by -1. Some asymmetry with respect to the sign of the bias current is clearly visible at nonzero fields. In conventional SQUIDs the maximum in the switching current always occurs at zero field [2] and the minimum occurs if the applied flux equals half of the flux quantum. However, this is not true in general in our nanowire SQUIDs. In this example of the representative Device

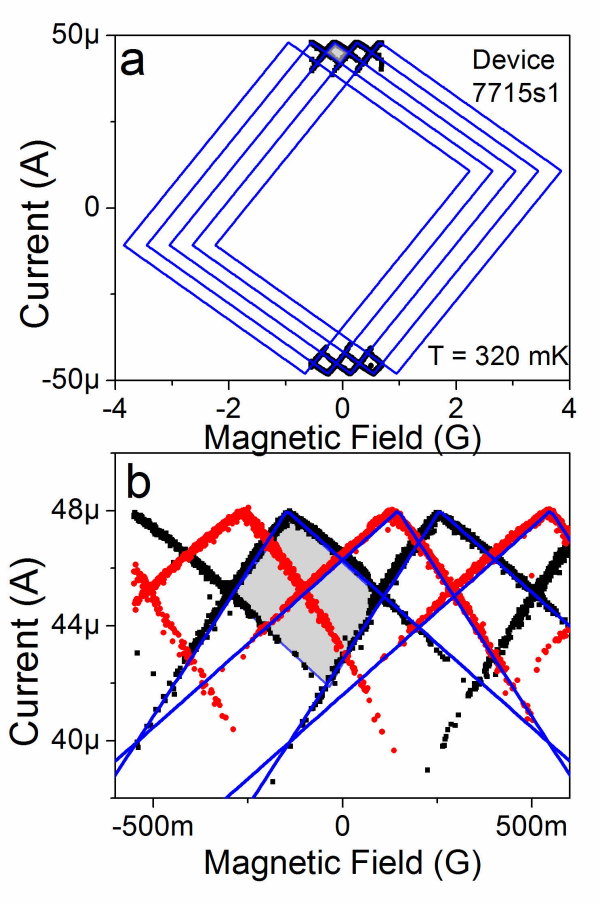

FIG. 3: a) The critical current (black points) plotted against magnetic field. Fits, in solid lines forming diamond shapes, show the Little-Parks diamonds generated by our model (see text). They predict the critical currents associated with states characterized by certain fixed vorticity values. From left to right, the vorticity of the fitting curves increments from n_v = -2 to 2. Fit parameters are listed in Table I. b) To compare positive and negative branches, the absolute value of the critical current and fits of the critical current for states n_v = 0 and 1 are plotted. Black squares denote positive critical currents and red circles denote the absolute value of the negative critical currents. The shaded area in both figures shows the positive-current "unique-vorticity diamond" for the state $n_v = 0$.

7715s1 measured at T =320 mK (Fig. 3b), one can see that $I_{C+} = I_{C-}$ at $B = 0$. Yet, neither the maxima nor the minima occur at $B = 0$. This happens because the kinetic inductance values are different for the two wires. To achieve the maximum supercurrent for the SQUID both wires need to achieve their critical currents simultaneously. Yet, as the external current is slowly ramped up the electric potential is the same at all points of each superconducting electrode. Thus, the phase difference is the same for both wires (unless there is a vortex in the loop). Yet, the supercurrent is smaller in the wire with the larger inductance (the kinetic inductance is dominant in very thin wires). This means the supercurrent will be lower in the longer wire if all other parameters are identical. Yet if the wires have the same diameter they have the same critical current. Thus when the shorter wire reaches the critical current the longer wire remains subcritical. Thus the maximum possible supercurrent cannot be achieved at zero field. But, if an appropriate magnetic field is applied, which generates an excess Meissner current in the loop, then both wires can come to their critical state simultaneously. At such a magnetic field the critical current of the device will be the maximum. For this to happen the Meissner current should be such that it reduces the total current in the shorter wire and increases the total current in the longer wire.

III. MODEL

The results can be understood as follows. The total bias current is split between the two wires. We assume the current in each individual wire is given by a linear current-phase relationship

$$I_j = I_{C,j}\phi_j/\phi_{C,j} \tag{1}$$

where j = 1 or 2 is the wire number. I_j is the supercurrent through the wire j, $I_{C,j}$ is the critical current of wire j, and ϕ_j is the difference of the phase of the complex superconducting order parameter taken between the end points of the wire j. We also use the concept of the critical phase $\phi_{C,j}$, which is the phase difference at which the supercurrent reaches its maximum possible value and the superconductivity gets destroyed. In long wires the critical phase is much greater than $\pi/2$. This is the case for our samples since our wires are much longer than the coherence length. The critical phase would be $\phi_C = \pi/2$, as in JJs, if the nanowires would be much shorter than the coherence length. But this is not the case since the coherence length is of the order of 10 nm in the samples discussed and the length is typically larger than 150 nm (the length for each wire is given above).

In this model, the critical current of each nanowire is assumed independent of the magnetic field because the wires are thin and the magnetic field is weak. To understand this recall that the applied field is much smaller than the field needed to create a single flux quantum through the area of a typical nanowire. Thus internal Meissner currents in the nanowire are negligible. The assumption of the independence of each nanowire critical current on the magnetic field is confirmed by the experimental observation that all maxima of the periodic critical current of the SQUID occur at the same current value. For example in Fig. 3b the red curve has three maximum and all of them occur at about 48 μA.

To complete the model we need to take into account that the order parameter must be single-valued. Hence,

the total phase around our superconducting loop must be an integer multiple of 2π. Therefore, the phases across each wire and the electrodes (i.e. on a closed trajectory around the loop) must add up as [17, 20]

$$\phi_1 - \phi_2 + 2\delta = 2\pi n_v \quad (2)$$

Here, the vorticity (the winding number) of the SQUID loop is n_v. The phase difference within each electrode $\delta = \delta(B)$ (defined between the ends of the two nanowires connected to the same electrode) is assumed to be the same on both the electrodes; thus, the factor of 2 occurs in the phase balance equation given above. This Meissner phase difference can be computed as $2\delta(B) = 2\pi(B/\Delta B)$, where ΔB is the Little-Parks period and B is the external field applied perpendicular to the SQUID loop [17]. Note that the model assumes that at zero field the phase gradient is zero in each electrode even if some external bias current is applied. This is motivated by the fact that the superconducting films are much stronger superconductors because they are wider and usually have a higher critical temperature. Thus the phase gradient in the electrodes is assumed to be negligibly affected by the supercurrents in the nanowires following the argument of Ref. [17].

In this simplified model only the kinetic energy of the superconducting condensate is taken into account and the magnetic field distortion by the Meissner effect is neglected. A more rigorous theoretical model might need to include the magnetic moment of the supercurrent in the loop and its interaction with the applied field [38, 39]. In the present model, the phase gradients in the electrodes are assumed to be created by the Meissner current only.

Combining equations 1 and 2, and the requirement that superconductivity should be destroyed if $\phi_j \geqslant \phi_{C,j}$ in any of the wires, we have calculated the total critical current of the nanowire SQUID for a given vorticity n_v and magnetic field B. We assume the total critical current of the device, $I_C(B)$, equals the smallest total applied current at which the current across either wire reaches its critical value. Different values of n_v result in different critical currents. When the critical current of a vorticity state n_v is plotted against magnetic field, we find the boundaries of the region in which the vorticity state n_v is stable, which are called Little-Parks (LP) diamonds because their periodicity corresponds to Little-Parks oscillations of the nanowire loop. Outside its LP diamond, the vorticity state n_v cannot exist because the critical current of at least one wire is exceeded according to the equations 1 and 2. When the system reaches the boundary of its vorticity state, either the vorticity of the system will change to a new, stable vorticity, by means of a phase slip, or the device switches to the normal state.

The critical currents of Device 7715s1 are calculated using equations 1 and 2 and shown in Fig. 3 by the straight lines. The fitting parameters are listed in Table I. The model gives good fits, thus confirming that the CPR is linear with a high accuracy. Many Little-Parks diamonds overlap over wide ranges of fields and currents. This explains why the critical current is multivalued (because the initial vorticity can be different). Another interesting fact is that the model does not involve the geometric inductance of the nanowires. Thus, only their kinetic inductance is essential. Therefore, it should be possible to reduce the dimensions of such nanowire SQUIDS by a large factor without compromising their performance (since the kinetic inductance can be large even if the wire is small, provided the critical current of the wire is small).

A linear or almost linear CPR has been predicted for thin and long wires at $T = 0$ [2, 21–23, 29, 30]. For example, in the limit of an infinite disordered wire the nonlinearity η, described by the equation $I_C/\phi_C = (1-\eta)\frac{dI}{d\phi}|_{\phi=0}$, is only about 2% according to Ref. [22]. And our nanowires qualify as disordered since they are amorphous and the mean free path is only about 3 Angstroms. Note that previously many computationally advanced models based on Ginzburg-Landau theory have been developed [25, 27, 28]. Yet, they are applicable to higher temperatures. Our goal is to address the low-temperature limit. Here, we have shown that a simple model based on a linear CPR provides excellent fits to our critical current data. Below, we will show how this model leads to a thorough understanding of the critical current vs magnetic field function, reveals the process by which the system switches from the superconducting state to the normal state, and how it correctly predicts the existence of hidden phase slips.

IV. ANALYSIS

According to our model, if the wires are different, the optimal vorticities (the one which produces the largest $I_C(B)$) are not always equal for positive and negative currents. At the largest currents at which the sample is still superconducting, only the optimal vorticity state is stable because for any other winding number the current would be larger than the critical current. The region in field and current in which the optimal vorticity is the only stable superconducting state will be referred to as the unique-vorticity diamond (UVD). The UVD is a region of the larger Little-Parks diamond which does not overlap with any other LP diamond. For example, the UVD for state $n_v = 0$ at positive currents of Device 7715s1 is shown as the shaded region in Fig. 3. If the system is superconducting within the unique vorticity diamond then the vorticity state is known. This suggests that nanowire SQUIDs may be applicable as memory devices using the unique-vorticity diamond to write a known vorticity state. At low current bias, the device can have

many different vorticity values, all except one of which are metastable. This metastability results in a multivaluedness of the critical current. It should be noted that the proposed model predicts the existence of many critical currents for a fixed field. Yet, experimentally, we cannot see all of them simply by measuring the critical current. This fact indicates that when the bias current reaches the critical current for a given vorticity state, the system is sometimes able to modify its vorticity without switching to the normal state. Thus, hidden phase slips can be predicted.

Each maximum in magnitude of $I_C(B)$ and the two critical current branches extending from it correspond to the critical currents associated with a particular vorticity state. We define a critical current branch as a continuous line segment of critical current when plotted versus magnetic field. The maximum itself occurs at the field when both wires reach their corresponding critical currents (and the critical phases) simultaneously. The reason that the crossing branches have different slopes is due to the fact that they represent different wires reaching their corresponding critical current and critical phase.

The critical phases (listed in Table I) are found to be approximately 20 radians in each device. Note that the critical phase of a Josephson junction is only $\phi_{CJJ} = \pi/2 = 1.57$ rad. If we would connect two Josephson junctions in series then we would need to apply a twice larger phase difference between the ends of the chain to achieve the phase difference of $\pi/2$ rad on each junction. Thus, the critical phase of a chain of two Josephson junctions connected in series would be $\phi_{CJJ} = \pi$ rad. If the chain contains three junctions in series then the critical phase is $\phi_{CJJ} = 3\pi/2 = 4.7$ rad. To have a critical phase of about 20 rad we would need to create a chain of about 13 JJs. Of course, our nanowires do not have Josephson junctions inside them, in the sense that there are no insulating barriers or weak links in them, since the wires are homogeneous. Yet every segment of size 2ξ can be considered as an independent region (junction) because a phase slip can occur within such a region. Note that the size of the phase slip core is 2ξ [40]. Thus, to estimate the critical phase, roughly, we can take the critical phase for one junction ($\phi_{CJJ} = \pi/2$) and multiply this by the number of independent segments (L/2ξ). Then the wire can be modeled as a chain of junctions of the total number $n_j = L/2\xi$. The critical phase for each junction is $\pi/2$. Thus the coherence length for a nanowire can be estimated from the equation $\phi_C \approx (\pi/2)(L/2\xi)$. If $\phi_C \approx 20$ rad (as seen in Table I) and L 200 nm then $\xi \approx$ 8 nm. This value of coherence length is consistent with those found in previous studies of $Mo_{75}Ge_{25}$ nanowires [41–43].

Standard Deviation: In measurements on superconducting junctions in which the current is slowly increased from zero, the measured switching current is typically slightly less than the true critical current of the junction [44]. The same phenomenon occurs in superconducting nanowires. Namely, as the bias current is swept up, thermal or quantum fluctuations (i.e., phase slips) can cause the nanowire to escape from the superconducting regime before the depairing current is reached [46]. Thus, thermal and/or quantum fluctuations cause a stochastic distribution of the switching current. In our model presented above we have treated the average switching current and theoretical critical current as if they are equal, for simplicity, because the fluctuations are small. Now we address the fluctuations of the switching current explicitly. In Fig. 4a we plot the switching currents of Device 31414s1 at 1.5 K as black points and the average switching current as a solid blue curve. The corresponding standard deviations of the switching current distributions are plotted in Fig. 4b. We choose to analyze the switching current distribution of Device 31414s1 because it turns out to be single-valued, i.e., it shows only one critical current branch at any magnetic field. While the switching current is stochastic due to thermal or quantum fluctuations, we do not see multiple clusters of switching currents at the same magnetic field which might be expected, for example, along the dotted blue lines in Fig. 4a.

To explain this single-valuedness consider the following argument. At 1.5 K, Device 31414s1 has a lower critical current than the other measured devices. The heat produced by single phase slips at lower branches of the critical current in Device 31414s1 is insufficient to produce a switching event and to drive the device normal. Rather, when the system is in a non-optimal vorticity state, a phase slip can transfer the system into a different vorticity state characterized by a higher critical current. This is because the heat released by a single slip is proportional to the value of the bias current.

For the purpose of the statistical analysis, the switching current is measured 300 times at each magnetic field. The average switching current is plotted in Fig. 4a as a solid blue line and the standard deviation σ of the switching current distribution is shown in Fig. 4b. We find, quite surprisingly, that there are regions in which the standard deviation does not depend on the magnetic field, while the mean value of the switching current changes with the magnetic field. In other words, the standard deviation of the switching current distribution is a periodic sequence of plateaus. Along each branch of the critical current, the standard deviation is constant. This fact gives us an important insight into the switching mechanism. As we will discuss below, these plateaus indicate that the switching events are initiated by phase slips in a single wire, namely the wire in which the critical current condition is reached first.

In order to understand the plots in Fig. 4, consider first the case in which a switching event occurs because the total current in wire 1 I_1 reaches its critical value $I_{C,1}$. Given that $I_1 = I_{C,1}$, the total applied current can

be calculated using Eq. 1, 2, and conservation of current. In the model, if one wire reaches the critical current then the entire SQUID reaches its critical current also. Therefore the total current calculated when $I_1 = I_{C,1}$ is the total critical current of the device. This calculated critical current of the SQUID changes linearly with magnetic field. Obviously, as long as switching events are caused by wire 1 reaching its critical current, the total current in wire 1, I_1, will always (i.e., at any magnetic field) equal its critical value $I_{C,1}$ if the critical current of the device is approached. Remember also that $I_{C,1}$ and $I_{C,2}$ are independent of the magnetic field in the range of fields we study. And, at the same time, the total current in wire 2 is sub-critical for the considered group of the switching events. In this case, the standard deviation of the switching current distribution is related to the rate of phase slips as a function of the total current in wire 1, and not of the total applied current. This rate does not change noticeably with magnetic field because when the switching happens the total current in wire 1 is near its critical current, at any value of magnetic field. Thus, as long as a switching event is caused by wire 1 reaching its switching current, σ is constant because σ is defined by the rate of phase slips near the critical current.

Another, alternative way to discuss the constant sigma is to conjecture that the fluctuations of the switching current originate from the critical current fluctuations caused by thermal energy fluctuations or quantum zero-point fluctuations. Since the critical current of each individual wire remains unchanged with magnetic field, its fluctuations remain unchanged also. Therefore, sigma remains unchanged as magnetic field is swept, as long as the phase slips causing the switching events occur in one particular nanowire.

In accord with the above discussion, σ will also be constant in the range of magnetic fields in which switching events are caused exclusively by wire 2 reaching its critical current. Such regions will be characterized by a different plateau since the rate of phase slips in wire 2 is different from wire 1, if the wires have different dimensions and/or critical temperature. Note that the critical temperature of the wire depends on its width as well as its thickness.

This explanation is based on the fact that there exist rather wide ranges of the magnetic field in which the switching of the device is always caused by a phase-slip in the same wire. Such field regions are characterized, also, by linear dependence of the switching current on the applied field. Indeed, each plateau in Fig. 4b (see red and blue guide-to-the-eye lines) is a region in magnetic field over which switching events of the entire device are all caused by one particular wire reaching its critical current.

We notice also that a dip in the standard deviation occurs at fields where the switching current is the minimum. Below we suggest an explanation for this dip. First, notice that, according to our model, at the minima of the mean switching current shown in Fig. 4a, there are two metastable vorticity states, n_v and $n_v + 1$. (This is unlike any other region in the solid blue curve of Fig. 4a, where there is just one metastable vorticity state and all others are unstable.) Thus, just below the $I_C(B)$ minimum, phase slips might not always cause a switching event. Rather, the vorticity can change without causing a switching event since the SQUID might transition between the two available metastable states.

Since we observe no switching events at currents below the switching current minima (e.g. along the blue dotted lines in Fig. 4a), we suggest that a single phase-slip in a non-optimal vorticity state does not produce enough heat to drive the system normal in Device 31414s1. Thus near the minima, where multiple vorticity states are metastable, we do not expect a single phase-slip to result in a switching event either. Therefore, a possible scenario to describe a switching event at a minimum in $I_C(B)$ is as follows. We begin with zero applied bias current through the device and a magnetic field corresponding to the minimum of the switching current. At the minimum of the switching current, wire 1 nears its critical current if the system is in state n_v while wire 2 nears its critical current if the system is in state $n_v + 1$. We will assume the systems starts with vorticity n_v. As the current is increased and approaches the critical current of the device, a phase slip occurs on wire 1 (which has a current near its critical value) and the vorticity of the SQUID changes to state $n_v + 1$. This phase slip does not cause a switching event and thus remains unregistered. However, now the current in wire 2 is near its critical value. So another phase slip occurs, returning the system to state n_v. This process repeats until the heat produced by phase-slips suppresses the critical current of the SQUID below the applied current, driving the system normal and creating a switching event.

What is special in this scenario is that some phase slips remain undetected. As will be argued below, in such a regime where multiple phase-slips are required to produce switching events, the dispersion of the switching current is reduced. Additionally, this scenario can only occur near the minima where two metastable vorticity states have similar critical currents. Thus it is supported by the fact that we do not see a multi-valued $I_C(B)$ function which would be represented by clusters of switching currents along the blue dotted lines in Fig. 4a.

We suggest that the dip in the standard deviation may be due to the switching caused my multiple phase slips. This means that single phase slips do not always cause switching. Yet a coincides or nearly coincidence of two or more phase slips in time can switch the SQUID to the normal state. Quantitative statistical analysis of the multiple phase slips regime is more complicated; it certainly goes beyond the Kurkijärvi model [44]. The analysis of multiple phase slip switching events was done numerically [46, 48]. One important result was that the stan-

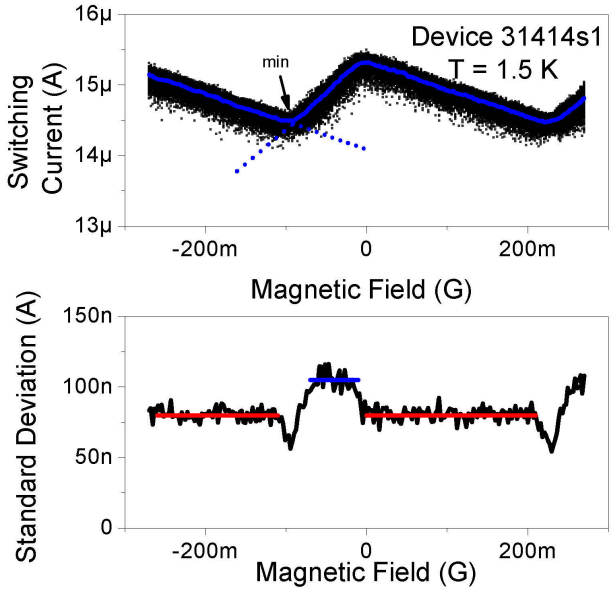

FIG. 4: a) The switching current vs magnetic field for Device 31414s1. Device 31414s1 only shows one critical current branch at each magnetic field, i.e., the $I_C(B)$ function is single-valued (however the switching current itself is stochastic due to thermal or quantum fluctuations). The mean switching current is plotted as a blue line. A minimum in the $I_C(B)$ function is denoted as "min". Dotted blue lines extend from this minimum as an example of where our model would predict phase slips to occur at non-optimal vorticities. b) The standard deviation of the switching distribution vs magnetic field is a periodic sequence of plateaus. Along each plateau, a switching event is caused by a particular wire reaching its critical current. Horizontal lines in red (at 80 nA) and blue (at 105 nA) have been plotted guide to the eye.

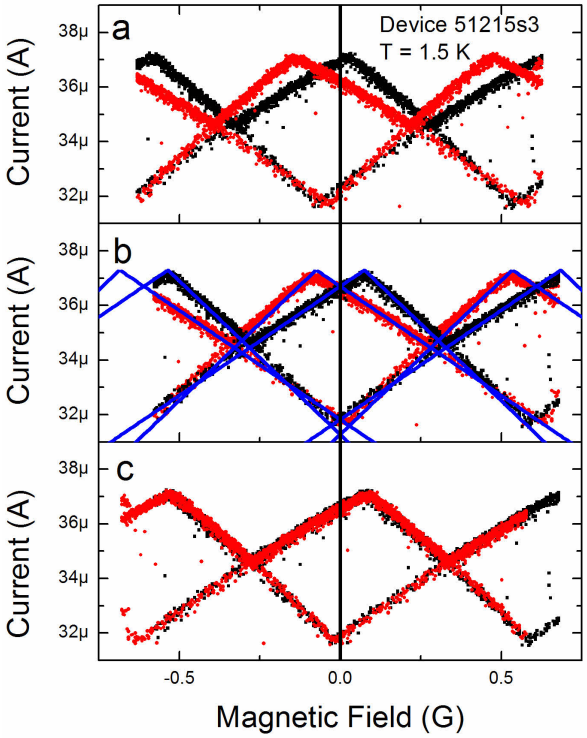

FIG. 5: a) Raw critical current data. The magnitudes of the positive critical current (black squares) and the negative critical current (red circles) are not equal at zero field (vertical black line). b) The entire critical current plot is shifted along the magnetic field axis such that the largest magnitude positive and negative critical currents are equal at zero field. Such shift compensates for the initial unaccounted offset magnetic field in the setup. This corrected data is fit to our model and the fits are shown in blue lines. Fit parameters are listed in Table I. c) The magnitude of the negative critical current is flipped about (mirror reflected) the vertical B = 0 line. The overlap of the black and red curves is consistent with the physical symmetry of the system: Reversing the direction of the current and the applied field at the same time should produce no change to the system.

dard deviation is reduced when multiple phase slips are needed to switch the device [46, 48], compared to the single phase slip switching, where each phase slip generates a switching event. Thus, we suggest that multiple phase slip switching process can explain the observed dips in the standard deviation plot, located at magnetic fields at which the switching current is the minimum.

Symmetry 1: A transformation consisting of reversing both the direction of applied current and the direction of the magnetic field will reproduce the initial untransformed state [15]. We illustrate the symmetry transformation on Device 51215s3, in Fig. 5. In Fig. 5a the raw critical current data is presented. We expect the positive critical current I_{C+} (black squares) and the negative critical current I_{C-}, multiplied by -1, (red dots) to be equal at zero magnetic field (for zero vorticity). This is not the case in the raw data, due to presence of an unaccounted offset magnetic field in the cryostat. The offset may be due to the Earth field or some other unaccounted sources, for example. Therefore in Fig. 5b we shift the data horizontally, along the B-axis, thus compensating for the unaccounted magnetic field. Now the positive (black) and the negative (red) branch of critical current (corresponding to the same vorticity $n_v = 0$) intersect at $B = 0$ (Fig. 5b). The fits (blue lines) produced by our model exhibit an excellent agreement with the data. In Fig. 5c the symmetry transformation is completed by multiplying by -1 the magnetic field value of each data point corresponding to the negative critical currents. Thus, modified negative branches (red) match perfectly well the corresponding positive branches (black) (see Fig. 5c). To summarize, the discussed current-field reversal symmetry can be expressed as $-I_{C-}(-B) = I_{C+}(B)$ where the critical current function is the complete multivalued function.

Symmetry 2: Now we discuss the position of the crossing points of the plots representing the magnitudes of the positive and negative critical currents. At inte-

ger flux quanta and half-integer flux quanta the positive critical current of some vorticity state n_{v+} and the negative critical current of the matching vorticity state n_{v-} are equal to each other in magnitude, i.e., $I_{C+}(B, n_{v+}) = -I_{C-}(B, n_{v-})$. For this to hold true, the vorticity states n_{v+} and n_{v-} must be related by $n_{v+} + n_{v-} = \text{int}(\frac{2B}{\Delta B}) = \text{int}(2\delta(B)/\pi)$ where ΔB is the period. Mathematically, magnetic fields of integer flux quanta can be expressed as $B = n\Delta B$ and half-integer flux quanta magnetic fields can be expressed as $B = (n + 1/2)\Delta B$. Here n is an integer. The experiment supports our conclusions: The magnitudes of the negative (red) and the positive (black) experimental critical current curves in Fig. 3b intersect at integer and half-integer flux quanta, i.e., at $B = n\Delta B$ and $B = (n + 1/2)\Delta B$. To derive this equality theoretically, we will consider the cases when the current through wire 1 reaches its positive critical value at $I_1 = I_{C,1}$ and when the current through wire 1 reaches its negative critical value at $I_1 = -I_{C,1}$. In these cases, the total current I_{Total} through the device (which is the total critical current of the device) can be written as

$$I_{Total} = I_{C+}(B, n_{v+}) = I_1 + I_2 = I_{C,1} + I_2 \tag{3}$$

for positive current and

$$I_{Total} = I_{C-}(B, n_{v-}) = I_1 + I_2 = -I_{C,1} + I_2 \tag{4}$$

for negative current. Here, n_{v+} and n_{v-} are two unknown vorticity states.

We can then calculate the current in wire 2, I_2, using Equations 1 and 2. At positive currents

$$I_2 = \frac{I_{C,2}}{\phi_{C,2}}(\phi_{C,1} + 2\delta - 2\pi n_{v+}) \tag{5}$$

and at negative currents

$$I_2 = \frac{I_{C,2}}{\phi_{C,2}}(-\phi_{C,1} + 2\delta - 2\pi n_{v-}). \tag{6}$$

Next, we multiply the negative total critical current by -1 and set it equal to the total positive critical current.

$$\begin{aligned} I_{C,1} + \frac{I_{C,2}}{\phi_{C,2}}(\phi_{C,1} + 2\delta - 2\pi n_{v+}) = \\ -(-I_{C,1} + \frac{I_{C,2}}{\phi_{C,2}}(-\phi_{C,1} + 2\delta - 2\pi n_{v-})) \end{aligned} \tag{7}$$

This reduces to

$$2\delta - 2\pi n_{v+} = -2\delta + 2\pi n_{v-} \tag{8}$$

or more simply,

$$n_{v+} + n_{v-} = \frac{2}{\pi}\delta. \tag{9}$$

Recall that δ, the phase difference between the ends of wire 1 and wire 2 within an electrode and is related to the magnetic field by $\delta = \pi B/\Delta B$ where ΔB is the period. Thus, we find that

$$n_{v+} + n_{v-} = \frac{2B}{\Delta B}. \tag{10}$$

For this equation to hold, $\frac{2B}{\Delta B}$ must be an integer (as the vorticity values must also be integers). Therefore, solutions exist only if $B = n\Delta B/2$ where n is an integer, i.e., when the magnetic field is either at an integer multiple of the period (and the flux is at an integer flux quanta) or when the magnetic field is at an integer plus one-half period (and the flux is at a half-integer value of flux quanta). Thus, the crossing points of the negative and positive critical currents are located at integer and half-integer fluxoid values for the nanowire SQUID.

This analysis considered positive total critical currents achieved when $I_1 = I_{C,1}$ and the total negative critical current when $I_1 = -I_{C,1}$. A similar analysis can be done considering the total positive critical current when $I_2 = I_{C,2}$ and the total negative critical current when $I_2 = -I_{C,2}$. The same result will be found. We therefore conclude that at integer flux quanta and half-integer flux quanta, for each positive critical current, there will be a negative critical current of equal magnitude and vice versa. This relationship can be written as

$$I_{C+}(B, n_{v+}) = -I_{C-}(B, n_{v-}) \tag{11}$$

where $n_{v+} + n_{v-} = \text{int}(\frac{2B}{\Delta B})$. In the general condition given above, the integer vorticity values n_{v+} and n_{v-}, which index the positive and the negative critical current branches respectively, may be equal or not equal. For example, at zero field $I_{C+}(B = 0, n_{v+} = 0) = -I_{C-}(B = 0, n_{v-} = 0)$ at the largest magnitude critical currents, but $I_{C+}(B = 0, n_{v+} = 1) = -I_{C-}(B = 0, n_{v-} = -1)$ is also true at a smaller magnitude critical current, meaning that there could be more than one crossing point at $B = 0$ in this example. To illustrate this conclusion, consider Fig. 3b where two crossing points are visible between the black curves and red curves at each period and half-period in magnetic field.

Shifts in the maxima: The maximum of the critical current deviates from zero field if the critical phases of the two wires are different. The maximum in $I_C(B)$ at zero vorticity occurs when the total critical current is equal to the sum of the individual critical currents of the wires, $I_C = I_{C,1} + I_{C,2}$. Thus, to achieve the maximum

the phase differences imposed on each wire must equal their critical phases. If the magnetic field is zero then the phases imposed on the wires are either equal to each other or differ by 2π if the number of phase slips passed through one wire is not equal to the number of phase slips passed through the second wire. This is because the phase gradient is assumed zero inside the electrodes, unless a nonzero magnetic field is applied. Thus, to achieve the maximum some magnetic field is needed to fine tune the phase difference on each wire to its critical value. To see this consider initially Equation 2 assuming the vorticity of the loop is zero and the phases of both wires are critical : $\delta(B) = \frac{1}{2}(\phi_{C,2} - \phi_{C,1})$. Obviously the phase difference induced by the magnetic field has to be nonzero if two critical phases are not equal. Recall that $\delta(B)$ is linearly proportional to B [17]. Thus, if the critical phases of the wires are not equal one has to apply a nonzero perpendicular field to achive the maximum possible supercurrent through the SQUID. The largest critical current at negative bias and zero vorticity can similarly be found when $\delta(B) = \frac{1}{2}(\phi_{C,1} - \phi_{C,2})$. Thus the largest positive critical currents and the largest negative critical currents of the state $n_v = 0$ are shifted from zero field in equal amounts, but opposite directions, and the magnitude of the shift is determined by the differences in the critical phases of the two wires.

Metastability: Using our model, we can calculate the conditions for which multiple vorticity states are metastable. For example, at zero field and zero current, if we assume the two wires are identical ($I_{C,1} = I_{C,2}$ and $\phi_{C,1} = \phi_{C,2}$) then $\phi_1 = -\phi_2$ (this is found using Eq. 1 and conservation of current) and Eq. 2 becomes

$$2\phi_1 = 2\pi n_v. \tag{12}$$

The value of ϕ_1 can range from $-\phi_{C,1}$ to $\phi_{C,1}$. Thus, the value of n_v at zero current and field can be any integer between $-\phi_{C,1}/\pi$ and $\phi_{C,1}/\pi$. So, as long as $\phi_{C,1}, \phi_{C,2} \geq \pi$, vorticity states $n_v = -1$, 0 and 1 will be stable at zero field and current. It has been shown that asymmetric SQUIDS composed of Josephson junctions can have multiple metastable vorticity states [49], however, this result is derived considering geometric inductance. Our nanowire loops depend on kinetic inductance rather than geometric inductance, making our analysis of the metastability of vorticity states qualitatively different from studies of traditional Josephson junction SQUIDs. Note that this analysis is performed assuming the CPR is linear which is not expected to be true for very short nanowires.

Hidden phase slips: Next, we demonstrate a method by which we can observe hidden phase slips which do not produce switching events. We begin with the Device 7715s1 in the superconducting state and in the unique vorticity diamond for state $n_v = 0$. Therefore we know the device must have a vorticity of zero as $n_v = 0$ is the only allowed superconducting state in the UVD for state $n_v = 0$. We drive the system to a value of current and field, which we call a testing point, and then return the system to the unique vorticity diamond of state $n_v = 0$. The testing point is chosen at different locations of the I-B (current-field) plane, progressively further from the UVD of the $n_v = 0$ state. If the testing point stays within the $n_v = 0$ Little-Parks diamond, i.e., the region where the vorticity $n_v = 0$ is stable, then as we return to the UVD we never detect a switching event. But, if the testing point reaches the boundary of the LP diamond then the vorticity changes somewhere near the testing point and either a switching event or a hidden phase slip occurs. If a hidden phase slip occurs, then the obtained vorticty n_v' does not equal 0. Upon returning to the UVD of state $n_v = 0$ from a state $n_v' \neq 0$, the system must cross the boundary of the LP diamond for n_v'. This boundary crossing results in a phase slip, which may cause a switching event. To ensure we detect when $n_v' = \pm 1$, we enter the UVD of state $n_v = 0$ at a magnetic field where the critical currents of both states $n_v = -1$ and $n_v = 1$ produce switching events (see Fig. 6). So to summarize, if the testing point is within the original LP diamond, then no switching events occur as we return to the starting point at the UVD. If the testing point reaches the LP diamond boundary, then we detect switching events either at this boundary or as we return to the starting point at the UVD with some probability above zero. Thus the boundaries of the LP diamond can be determined, even in regions where there is no switching at the boundary and only hidden phase slips occur.

If at any point, the system switches to the normal state, either upon reaching the testing point or returning to the unique vorticity diamond, we record the testing point as a boundary of state $n_v = 0$. This process is repeated for states $n_v = -1$ and $n_v = 1$. Results are shown in Fig. 6. Black points are the critical currents. Green, red and blue points are the testing points which correspond to the borders of vorticity states $n_v = -1, 0$ and 1. Solid lines show theoretical fits and fitting parameters are listed in Table I. We find that the boundaries of each vorticity states matches theoretical predictions. Thus, we are able to observe signatures of phase slips which do not produce switching events (at low currents) and confirm the accuracy of our model.

We can also determine the positive and negative UVDs of the same vorticity state. If the effects of external magnetic fields (due to, for example, the Earth) are not precisely known, then we do not know which of the crossing points discussed above (see Section Symmetry 2) correspond to zero field, and which correspond to integer or half-integer flux quanta. Additionally, while we know from the discussion of shifts in the maxima that the peaks in the positive and negative critical currents are shifted from zero in equal and opposite directions, this does not exactly determine which pair of extrema correspond to

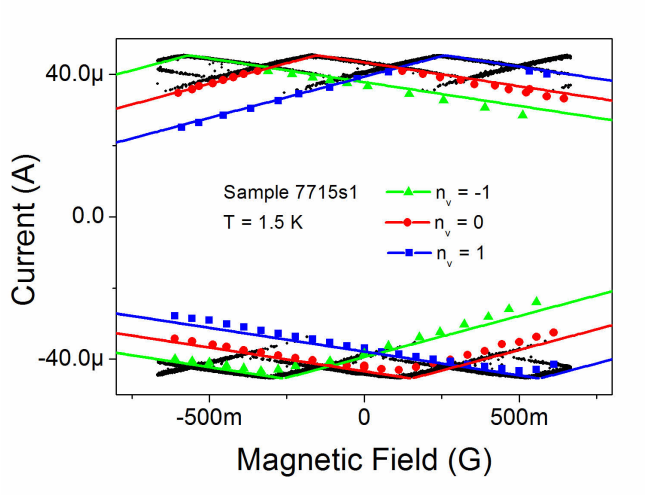

FIG. 6: The borders of vorticity states (Little-Parks diamonds) $n_v = -1$, 0 and 1 for Device 7715s1 are found experimentally as described in the text and are plotted as green, red and blue points (testing points where a change of the vorticity first occurs). Solid lines show theoretical fits of the vorticity stability regions. Black points show the switching currents.

Device	I_{C1} (μA)	I_{C2} (μA)	ϕ_{C1} (rad)	ϕ_{C2} (rad)
7715s1 (at T = 0.3 K)	16.9	31.1	23.6	21.1
7715s1 (at T = 1.5 K)	15.9	29.5	21.9	19.4
51215s3	21.5	15.8	19.6	20.4
31414s1	10.0	5.3	19.8	23.9

TABLE I: Fitting Parameters. The fitting parameters for our linear CPR model of nanowires include the critical currents of each wire, I_{C1} and I_{C2}, and the critical phase of each wire, ϕ_{C1} and ϕ_{C2}.

the $n_v = 0$ state. Thus an algorithm to characterize which UVDs correspond to the same vorticity state may be desirable. This algorithm can be the same algorithm by which hidden phase-slips are detected, using a starting point in some UVD at positive currents, and a testing point in a UVD at negative currents. If the trajectory of the system in the B-I plane does not cross any boundaries of the LP diamond of the initialized vorticity state, no switching events will be detected. Therefore if the system can be brought back and forth between a pair of positive and negative UVDs many times without any switching events, then this pair can be assumed to correspond to the same vorticity state. If a switching event does occur, this pair must not correspond to the same vorticity state.

V. CONCLUSIONS

In conclusion, nanowire SQUIDs are qualitatively different from conventional SQUIDs because the critical phase of the nanowires involved is much larger than $\pi/2$. The critical current is multivalued. At integer flux quanta and half-integer flux quanta, the magnitudes of the positive and negative critical currents are equal, but are not necessarily maxima or minima. The stability regions of vorticity states are described by Little-Parks diamonds, and the critical current function is composed of linear segments. We find that a linear segment in the critical current vs magnetic field function corresponds to a plateau in the standard deviation in the switching current distribution. A single line segment / plateau corresponds to the situation where the current in one wire reaches its critical current for some vorticity state and the switching always happens in the same wire. We propose a new model to describe the multivalued function of the critical current on the magnetic field. The model is applicable at temperatures much lower than the critical temperatures of the nanowires. We use the model to predict hidden phase slips at relatively low bias current values, where phase slips do not cause switching events. We propose an algorithm allowing the detection of the occurrence of hidden phase slips, which follow the Little-Parks diamonds corresponding to the vorticity stability limits. We test our model by detecting hidden phase slips which do not produce switching events along predicted boundaries of vorticity states. Future work will be focused on the macroscopic quantum tunneling effects, especially for case of the hidden phase slips.

We thank D. Averin and J. Ku for helpful discussions. This work was supported by the National Science Foundation under the Grant No. ECCS-1408558.

[1] R.C. Jaklevic, J. Lambe, H. Silver, and J.E. Mercereau, *Phys. Rev. Lett.* **12**, 159 (1964).
[2] M. Tinkham, *Introduction to Superconductivity*, 2nd ed. (McGraw-Hill, New York, 1996).
[3] A. N. McCaughan, Q. Zhao and K. K. Berggren, *Sci. Rep.* **6**, 28095 (2016).
[4] D. Vasyukov *et al.*, *Nature Nanotech.* **8**, 639 (2013).
[5] O. J. Sharon, A. Shaulov, J. Berger, A. Sharoni and Y. Yeshurun, *Sci. Rep.* **6**, 28320 (2016).
[6] I. Petković, A. Lollo, L. I. Glazman and J. G. E. Harris, *Nat. Comm.* **7**, 13551 (2016).
[7] R. Monaco, J. Mygind, R. J. Rivers and V. P. Koshelets, *Phys. Rev. B* **80**, 180501 (2009).
[8] R. Vijay, E. M. Levenson-Falk, D. H. Slichter and I. Siddiqi, *Appl. Phys. Lett.* **96**, 223112 (2010).
[9] S. Michotte, D. Lucot and D. Mailly, *Phys. Rev. B* **81**, 100503 (2010).
[10] O. Bourgeois, S. E. Skipetrov, F. Ong and J. Chaussy, *Phys. Rev. Lett.* **94**, 057007 (2005).
[11] S. Adam, X. Hallet, L. Piraux, D. Lucot and D. Mailly, *Phys. Rev. B* **84**, 104512 (2011).
[12] B. Pannetier, J. Chaussy, R. Rammal and J. C. Villegier, *Phys. Rev. Lett.* **53**, 1845 (1984).
[13] R. Arpaia, M. Arezo, S. Nawaz, S. Charpentier, F. Lombardi and T. Bauch, *Appl. Phys. Lett.* **104**, 072603 (2014).

[14] V. L. Gurtovoi, S. V. Dubonos, S. V. Karpii, A. V. Nikulov and V. A. Tulin, *J. Exp. Theor. Phys.* **105**, 262 (2007); V. L. Gurtovoi, S. V. Dubonos, A. V. Nikulov, N. N. Osipov and V. A. Tulin, *J. Exp. Theor. Phys.* **105**, 1157 (2007).

[15] A. A. Burlakov, V. L. Gurtovoi, A. I. Il'in, A. V. Nikulov and V. A. Tulin, *JETP Lett.* **99**, 169 (2014).

[16] V. L. Gurtovoi *et al.*, *J. Exp. Theor. Phys.* **113**, 678 (2011).

[17] D. S. Hopkins, D. Pekker, P. M. Goldbart and A. Bezryadin, *Science* **308**, 1762 (2005).

[18] A. Belkin, M. Belkin, V. Vakaryuk, S. Khlebnikov and A. Bezryadin, *Phys. Rev. X* **5**, 021023 (2015).

[19] R. F. Voss, R. B. Laibowitz and A. N. Broers, *Appl. Phys. Lett.* **37**, 656 (1980).

[20] D. Pekker, *et al.*, *Phys. Rev. B* **72**, 104517 (2005).

[21] J. Bardeen, *Rev. Mod. Phys.* **34**, 667 (1962).

[22] Yu. Kupriyanov and V. F. Lukichev, *Fiz. Nizk. Temp.* **6**, 445 (1980) [*Sov. J. Low Temp. Phys.* **6**, 210 (1980)].

[23] K. K. Likharev, *Rev. Mod. Phys.* **51**, 101 (1979).

[24] W. Wernsdorfer *et al.*, *Phys. Rev. Lett.* **79**,4014 (1997).

[25] K. Hasselbach, D. Mailly and J. R. Kirtley, *J. Appl. Phys.* **91**, 4432 (2002).

[26] D. Harza, J. R. Kirtley and K. Hasselbach, *Appl. Phys. Lett.* **103** 093109 (2013).

[27] A. G. Sivakov, A. S. Pokhila, A. M. Glukhov, S. V. Kuplevakhsky and A. N. Omelyanchouk, *Low Temp. Phys.* **40**, 408 (2014).

[28] G. J. Podd, G. D. Hutchinson, D. A. Williams and D. G. Hasko, *Phys. Rev. B* **75**, 134501 (2007).

[29] P. F. Bagwell, *Phys. Rev. B* **49**, 10 (1993).

[30] T.-C. Wei and P. M. Goldbart, *Phys. Rev. B* **80** 134507 (2009).

[31] D. Meidan, Y. Oreg and G. Refael, *Phys. Rev. Lett.* **98**, 187001 (2007).

[32] W. A. Little and R. D. Parks, *Phys. Rev. Lett.* **9**, 9 (1962).

[33] R. D. Parks and W. A. Little, *Phys. Rev.* **133**, A97 (1964).

[34] A. Bezryadin, Superconductivity in Nanowires (2013).

[35] A. Bezryadin, *J. Phys.: Condens. Matter* **20**, 043202 (2008).

[36] D. J. Weir *et al.*, *J. Phys.: Condens. Matter* **25**, 404207 (2013)

[37] C. Granata, E. Esposito, A. Vettoliere, L. Petti and M. Russo, *Nanotech.* **19**, 275501 (2008).

[38] A. Nikulov, Quantum Stud.: Math. Found. v. 3, p. 41-55 (2016).

[39] V. L. Gurtovoi and A. V. Nikulov, *Phys. Rev. B* **90**, 056501 (2014).

[40] P. G. De Gennes, *Superconductivity of Metals and Alloys* (Westview Press 1999).

[41] A. Rogachev, T.-C. Wei, D. Pekker, A. T. Bollinger, P. M. Goldbart and A. Bezryadin, *Phys. Rev. Lett.* **97**, 137001 (2006).

[42] A. Belkin, M. Brenner, T. Aref, J. Ku and A. Bezryadin, *Appl. Phys. Lett.* **98**, 242504 (2011).

[43] J. Draskovic *et al.*, *Phys. Rev. B* **88**, 134516 (2013).

[44] J. Kurkijärvi, *Phys. Rev. B* **6** 832 (1972).

[45] W. A. Little, *Phys. Rev.* **156**, 396 (1966).

[46] M. Sahu *et al., Nat. Phys.* **5** 503 (2009).

[47] T. Aref *et al., Phys. Rev. B* **86** 024507 (2012).

[48] N. Shah, D. Pekker and P. Goldbart, *Phys. Rev. Lett.* **101** 207001

[49] W.-T. Tsang and T. V. Duzer, *J. Appl. Phys.* **46**, 4573 (1975).